Journal of Hydrology 420–421 (2012) 205–215

Contents lists available at SciVerse ScienceDirect

Journal of Hydrology

journal homepage: www.elsevier.com/locate/jhydrol

Development and testing of a distributed urban storm runoff event model with a vector-based catchment delineation

H. Amaguchi [a,*], A. Kawamura [a], J. Olsson [b], T. Takasaki [c]

[a] Department of Civil and Environmental Engineering, Graduate School of Urban Environmental Sciences, Tokyo Metropolitan University, 1-1 Minami-Ohsawa, Hachioji, Tokyo 192-0397, Japan
[b] Research & Development (Hydrology), Swedish Meteorological and Hydrological Institute, 601 76 Norrköping, Sweden
[c] Civil Engineering Center, Tokyo Metropolitan Government, 1-19-15 Shinsuna, Koto-ku, Tokyo 136-0075, Japan

ARTICLE INFO

Article history:
Received 5 April 2011
Received in revised form 28 November 2011
Accepted 1 December 2011
Available online 9 December 2011
This manuscript was handled by Geoff Syme, Editor-in-Chief

Keywords:
Vector-based catchment delineation
Urban storm runoff event model
Tokyo Storm Runoff model
Urban hydrology
Urban landscape GIS delineation

SUMMARY

The recent advances in GIS technology as well as data availability open up new possibilities concerning urban storm runoff modeling. In this paper, a vector-based distributed storm event runoff model – the Tokyo Storm Runoff (TSR) model – is developed and tested for urban runoff analysis using two historical storm events. The set-up of this model is based on urban landscape GIS delineation that faithfully describes the complicated urban land use features in detail. The flow between single spatial elements is based on established hydraulic and hydrological models with equations that describe all aspects of storm runoff generation in an urban environment. The model was set up and evaluated for the small urban lower Ekota catchment in Tokyo Metropolis, Japan. No calibration or tuning was performed, but the general model formulation was used with standard parameter values obtained from the literature. The runoff response to two storm events were simulated; one minor event resulting only in a small-scale flood wave and one major event which inundated parts of the catchment. For both events, the simulated water levels closely reproduced the observed ones. For the major event, also the reported inundation area was well described by the model. It was also demonstrated how the model can be used to evaluate the flow conditions in specific components of the urban hydrological system, which facilitates e.g. evaluation of flood-preventive measures.

1. Introduction

In recent years, a number of cases of urban flooding due to sewage system outflow and river overflow have occurred in Japan. In 1999, heavy storms lead to severe flooding particularly in the cities of Tokyo and Fukuoka, resulting in casualties and damages to more than 4000 houses (Kusuda, 1999; Goto, 2000). In 2000, extreme rainfall associated with a typhoon caused devastating flooding in the city of Nagoya, damaging over 60,000 houses (Yamamoto and Iwaya, 2002). Partly as a consequence of these and similar cases, a part of the Japanese flood defense legislation was amended in 2001 to require the publication of maps showing urban areas prone to flooding. Further, a flood damage countermeasure act for specified urban rivers was enforced in 2004. By this act, cities are required to have an urban catchment-based flood warning system which integrates all components contributing to urban runoff including hard and soft countermeasures. Examples of structural measures, currently recommended by the Tokyo Metropolitan Government, include local storage tanks, infiltration facilities and porous asphalt for roads.

Also in a more global perspective, a growing number of floods in urban areas is evident (e.g. Szöllösi-Nagy and Zevenbergen, 2004) and the problem of urban flooding is further expected to increase in the future. One obvious reason is today's rapid urbanization in many parts of the world, which is not always accompanied by a sufficient increase of the sewage system capacity. Another somewhat more speculative reason is the increased frequency of high rainfall intensities as a consequence of heat island phenomena and climate change, which has been indicated in several studies (IPCC, 2007; Bornstein and Lin, 2000). In response to the perceived and expected problems, urban flood management by structural and non-structural measures is an important strategy in many countries (Andjelkovic, 2001; Genovese, 2006). To properly evaluate the damage-reducing effects of current or planned structural measures (such as infiltration and storage facilities or permeable pavements), storm runoff models are required that take full advantage of today's geographical data sources and processing tools. A highly explicit and spatially distributed strategy in urban catchment modeling is crucial for accurately evaluating the

* Corresponding author. Tel.: +81 0426772779; fax: +81 0426772787.
E-mail address: amaguchi@tmu.ac.jp (H. Amaguchi).

0022-1694/$ - see front matter © 2011 Elsevier B.V. All rights reserved.
doi:10.1016/j.jhydrol.2011.12.003

effectiveness of various measures and for facilitating stakeholder communication.

From a process description point of view, watershed models for different purposes can be classified into lumped and distributed models (Singh, 1995). In most lumped models (e.g. HEC-1 (HEC, 1998), tank model (Sugawara, 1974) and SSARR (Spears, 1995)), some processes are described by simplified hydraulic laws, and other processes are expressed by empirical algebraic equations. Distributed models take an explicit account of spatial variability of processes, inputs, boundary conditions and watershed characteristics. In most distributed models, raster-based approaches for land-use characterization using digital elevation model (DEM) have been developed (e.g. SHE (Abbott et al., 1986a,b) and TOPMODEL (Beven et al., 1984)). Advantages of grid-based distributed models are their simple model structure and their use of catchment information which is generally readily available. Especially in urban applications, direct runoff in each grid is usually calculated on the basis of runoff coefficients or estimated fractions of impervious area in different land use categories (e.g. Niehoff et al., 2002; Choi and Ball, 2002; Park et al., 2008). A proper representation of land use is particularly crucial for accurate runoff simulation in urban environments, with their high degree of imperviousness (Leopold, 1968). In a grid-based rainfall runoff model, the parameters are generally either estimated from raster-based land-use maps of the city or from air photos, depending on the availability in the particular catchment, or by tuning them in model calibration and validation. While fast and practically convenient, the approach is limited in different respects. One is that the information on land-use maps may not be directly translatable into key hydrological characteristics such as permeability. Another limitation is that it is difficult with the grid-based models to evaluate local flood preventive measures together with the existing urban structures (buildings, roads, etc.) in a straight-forward way.

The recent advances in GIS technology as well as data availability open up new possibilities concerning urban storm runoff modeling. A few non-raster-based models have been developed from the view point of urban morphology in order to consider individual features in the urban environment. Sample et al. (2001) used GIS to facilitate urban storm water analysis by using land-use parcel boundaries (apartment, commercial, low- and medium-density residual and school). Rodriguez et al. (2003) proposed a vector-based catchment description based on information in so-called urban databanks, which includes categories cadastral parcel, building, street, sewer system and river, to calculate urban unit hydrographs. Rodriguez et al. (2008) employed the same concept to develop an urban water budget model.

In contrast to current modeling approaches, which are generally based on gridded data (e.g. Hsu et al., 2000; Ettrich et al., 2005; Dey and Kamioka, 2007), in this study we propose a new approach to simulate urban storm runoff and flood inundation with a vector-based catchment description. Vector-based data are potentially very useful for urban hydrological modeling, as a detailed and accurate representation of the catchment plays an important role in urban storm runoff simulations. The main novelty of this approach is that GIS is used to divide the urban environment into its smallest, perfectly homogeneous, elements which are hydraulically connected and finally integrated to form a complete catchment-based rainfall–runoff model. One key advantage of the detailed delineation is that flow tracking is possible on an element-to-element basis. Another advantage is that small, individual facilities that may strongly affect flow locally, such as infiltration areas or rainwater collection tanks of single buildings, may be reproduced. Thus detailed what-if scenarios of the consequences of some flow-preventive measure may be evaluated, both widespread implementation of some small-scale structure (e.g. local infiltration or green roofs) and single implementation of some large-scale construction (e.g. retention pond).

In this paper, an event-based urban storm runoff and flood inundation model is developed and applied for urban runoff analysis: the Tokyo Storm Runoff (TSR) model. The set-up of this model is based on what we term "urban landscape GIS delineation" (see Section 2.1). In the TSR model, surface flows as well as river and sewer flows are simulated by the unsteady flow equation considering inundated conditions. Infiltrated water from pervious land use elements finally drains out into the river as long-term groundwater runoff, which is however at present not considered in the TSR model. Neither does the TSR model presently represent evapotranspiration, time variable infiltration and subsurface flow. The model is therefore applied for event-based rainfall–runoff simulation in a dense urban catchment with minimal groundwater contributions to runoff and a well-maintained drainage infrastructure. In this study, the TSR model is set up for an urban sub-catchment of the Kanda River (Tokyo, Japan) and applied to test the runoff response to two actual storm events in 2005, one of which flooded part of the sub-catchment.

2. The Tokyo Storm Runoff (TSR) model

2.1. Urban landscape GIS delineation

Fig. 1 shows an example of the urban landscape GIS delineation for an urban catchment. The delineation first divides the catchment into two components: surface and subsurface. The surface component, which includes everything seen on a surface map, is in turn classified into block, road and river elements. Inside blocks, in order to calculate direct local runoff, further division is made into individual land use surfaces with different permeability such as building, paved area and grass. The subsurface component comprises sewer elements. Individual elements are further divided into segments, which is the smallest spatial calculation unit used in the TSR model. The spatial extent of a surface segment plays an important role in storm runoff simulation because properties such as elevation and water depth are averaged over this extent. In order to consider the differences between road and block altitudes the TSR model is supposed to use at least 5 m resolution DEM with 0.1 m precision in altitude.

2.2. Storm runoff process conceptualization

Fig. 2 shows a schematic of the rainfall–runoff process as represented in the TSR model. The models used here are composed of two analytical models; a hydrological model which simulates direct runoff from rainfall, and a hydraulic model which describe flows in blocks, roads, sewer, and river flows. In urbanized areas,

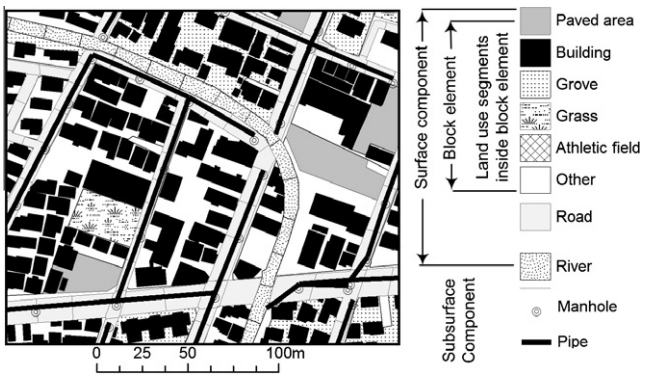

Fig. 1. Urban catchment modeling based on the urban landscape GIS delineation.

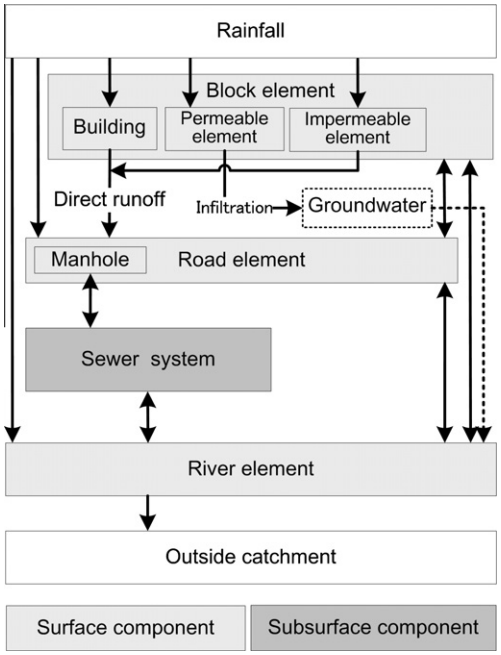

Fig. 2. Schematic of the rainfall–runoff process of the TSR model.

the main contribution to the catchment's response originates from water flows on the impervious surface component and in the subsurface component. Effective rainfall is calculated based on the permeability of the surface considering initial loss and final infiltration capacities (Toyokuni and Watanabe, 1986; Ando et al., 1986). The drainage system between the surfaces and the sewer system is based on a concept called "dual drainage", where urban drainage is modeled as two dynamically interconnected networks, and manholes function as points of flow exchange between them (Smith, 1992, 2006). Direct flow from a building segment to a road segment is simulated by a kinematic wave model, surface flow and river flow by the unsteady flow equation, and sewer pipe flow by the Preissman slot model (Preissmann and Cunge, 1961).

When rainfall begins, water falling on land use segments inside a block or a road forms pools, whereas water falling on a river adds to the river discharge. Rainfall excess from blocks flows out directly or indirectly through different types of surfaces and finally out into the road. When a manhole exists inside the surface, water flows through it to the rainwater sewer pipe conduit. In a manhole, the water level is obtained considering the inflow from the surface together with the upstream inflow from connected pipe conduits. In a pipe conduit, the water flow is obtained considering the water levels in the manholes located upstream and downstream, respectively. When the water level in a manhole exceeds ground level, water flows out and inundates the associated surface segment. The inundated water flows to adjacent surface segments until a manhole that has not reached full inflow capacity is found. The water in the sewer pipe conduits eventually reaches the river channel, which finally drains in the catchment outlet.

2.3. TSR model equations

2.3.1. Direct runoff

For practical estimation of rainfall excess, initial loss and continuing constant loss rate method (Pilgrim and Cordery, 1992) is used. Impervious surface includes land use classes building, road and parking lot, whereas classes grove, grass and athletic field are considered pervious. In an impervious surface, the only rainfall loss is the initial loss, which is mainly depression storage (Ando et al., 1986). Rainfall onto an impervious surface becomes effective after it exceeds the initial loss. It is expressed mathematically as

$$r_e(t) = \begin{cases} 0 & (\sum r(t) \le L_i) \\ r(t) & (\sum r(t) > L_i) \end{cases} \quad (1)$$

where $r(t)$ denotes rainfall intensity at time t (s), $r_e(t)$ effective rainfall rate (m/s), $\sum r(t)$ cumulative rainfall (m) and L_i initial rainfall loss for land use class i (m). Fig. 3 shows the schematic of urban landscape GIS delineation and the assumed flow processes. In land use segments inside block elements, direct runoff from a non-building segment to an adjacent block segment is assumed. The direct runoff on a building segment is as follows. Although rainfall on buildings usually runs off to the sewer system through a gutter, it is rare to have information on the connection between a building and the sewer system. In the TSR model, the kinematic wave model (Singh, 1996) is applied to calculate the flow from a building segment to the nearest road or river segment (Eqs. (2) and (3)). Since the actual shapes of individual buildings are sometimes complicated, the shape (flow distance x_b and flow width B) is supposed to be square with the same size as the actual segment.

$$\frac{\partial h_b}{\partial t} + \frac{\partial q_b}{\partial x_b} = r_e \quad (2)$$

$$q_b = \alpha h_b^{\beta} \quad \left(\alpha = \sqrt{\sin\theta}/\mathrm{N}_b, \quad \beta = 5/3\right) \quad (3)$$

where q_b denotes the discharge per unit width from the building (m^2/s), h_b the flow depth (m) and x_b the distance along the building (m). In (3), α and β are constants related to slope and surface roughness, $\theta$the slope of the building (rad) and N_b is the equivalent Manning's roughness coefficient ($s/m^{1/3}$).

On a pervious surface, rainfall losses consist of an initial loss L_i and an infiltration loss I_i for each land use class i (Ando et al., 1986). The initial loss L_i is equivalent to the sum of initial infiltration loss and depression storage. After the cumulative rainfall amount exceeds the initial loss, rainfall intensities in excess of the final infiltration capacity become effective. Therefore, the rainfall excess rate for a certain land use class is expressed as follows:

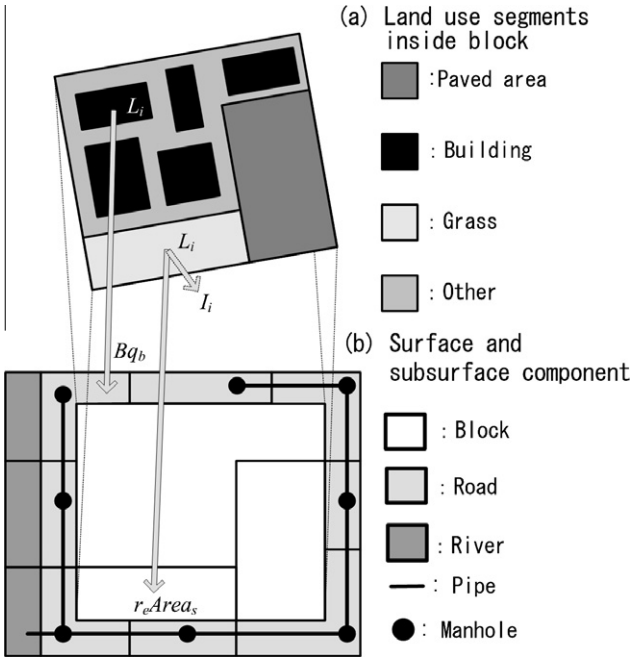

Fig. 3. Direct runoff process of the land use segment inside block element.

$$r_e(t) = \begin{cases} 0 & (\sum r(t) \le L_i) \\ r(t) - I_i & (\sum r(t) > L_i) \end{cases} \quad (4)$$

2.3.2. Surface flow

To calculate the discharge in surface component, one-dimensional unsteady flow without convective acceleration is assumed according to Eq. (5). Water level changes in the surface segments are computed by considering the effective rainfall and outflow/inflow from manhole elements in addition to the outflow/inflow from surface segments. After calculating water storage, the water depth is obtained by Eq. (6) (Fig. 4).

$$\frac{\partial Q_s}{\partial t} + gA_s\frac{\partial H_s}{\partial x_s} + \frac{gn_s^2 Q_s|v_s|}{R_s^{4/3}} = 0 \quad (5)$$

$$\frac{dh_s}{dt} = \frac{\Sigma Q_s + \Sigma B q_b + \Sigma Q_{div} + r_e Area_s}{Area_s} \quad (6)$$

where Q_s is the surface discharge (m^3/s), A_s the surface flow cross sectional area (m^2), H_s ($=z_s + h_s$) the surface water level (m), z_s the surface elevation (m), h_s the surface water depth (m), x_s the longitudinal distance along surface segment (m), n_s the surface Manning's roughness coefficient ($s/m^{1/3}$), v_s the velocity of surface flow (m/s), R_s the surface hydraulic radius (m), B the width of building segment (m), Q_{div} the discharge to/from manhole from/to surface (m^3/s) and $Area_s$ the surface area (m^2) (excluding the building area in block segments). The numerical analysis technique used for the surface flow, as well as for the calculations of sewer pipe flow and river flow described below, is the unsteady flow equation by the explicit finite difference method (Balloffet, 1969) used with the leapfrog calculation method (Dronkers, 1969).

2.3.3. Sewer pipe flow

The runoff in a sewer is usually in the state of free surface flow. However, in the case of a storm, both free surface flow and surcharged flow occur, and their regions vary temporally and spatially. In order to describe these processes in detail, a particular model for sewer pipe flow with surcharge is required and here dynamic waves are used to describe both free surface flow and surcharged flow. For the surcharged flow, the technique based on the assumption of a hypothetical slot is applied (Preissmann and Cunge, 1961). Fig. 4 shows the variables used in the calculation. In a pipe segment, the water flow is obtained considering the water levels in the manholes located upstream and downstream, respectively. The equation of motion without convective acceleration and continuity of the slot model is applied as

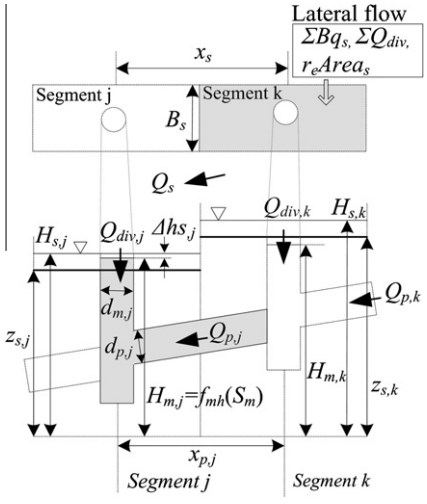

Fig. 4. Variables used in the surface and sewer flow.

$$\frac{\partial Q_p}{\partial t} + gA_p\left(\frac{\partial H_m}{\partial x_p}\right) + \frac{gn_p^2 Q_p|v_p|}{R_p^{4/3}} = 0 \quad (7)$$

where Q_p is the pipe discharge (m^3/s), A_p the pipe flow cross sectional area (m^2), H_m the manhole water level (m), x_p the distance along pipe (m), n_p the pipe Manning's roughness coefficient ($s/m^{1/3}$), v_p the velocity of pipe flow (m/s), R_p the pipe hydraulic radius (m).

In a manhole, the storage quantity and water level are calculated by Eqs. (8) and (9) respectively. The storage is based on the size of the manhole and its upward connection (Fig. 4) according to

$$\frac{dS_m}{dt} = \sum Q_{div} + \sum Q_m \quad (8)$$

$$H_m = f_{mh}(S_m) \quad (9)$$

where S_m is storage quantity in a manhole and connected pipe (m^3), Q_m the flow from/to the connected pipe (m^3/s) and f_{mh} a function relating storage to water level in the manhole (m).

When the water level in a manhole exceeds ground water level, water flows out and inundates the associated surface segment. The discharge between a manhole and a surface segment is evaluated according to

$$Q_{div} = \begin{cases} \frac{f_{mv}(H_m) - f_{mv}(H_s)}{dt} & (\text{outflow from manhole}) \\ \mu Area_m\sqrt{g\Delta h_s} & (\text{inflow to manhole}) \end{cases} \quad (10)$$

where f_{mv} is a function relating manhole water level to volume, μ a coefficient and $Area_m$ the manhole area.

2.3.4. River flow

The river channel flow considering the inflow from the rainfall and sewer pipes, as well as the side inflow from surface segments, is calculated by the equations of motion and continuity as

$$\frac{\partial Q_r}{\partial t} + \frac{\partial (Q_r^2/A_r)}{\partial x_r} + gA_r\frac{dH_r}{dx_r} + g\frac{n_r^2 Q_r|v_r|}{R_r^{4/3}} = 0 \quad (11)$$

$$\frac{\partial A_r}{\partial t} + \frac{\partial Q_r}{\partial x_r} = q_r \quad (12)$$

where v_r is the velocity of the river flow (m/s), x_r the distance along river channel (m), H_r the river water level (m), n_r river Manning's roughness coefficient ($s/m^{1/3}$), R_r the river channel hydraulic radius (m), A_r the river flow cross sectional area (m^2) and q_r the cumulative discharge from sewer system and surface segments to river segment in addition to rainfall (m^3/s).

3. Model application to the lower Ekota catchment

The study area selected for the model application is a small urban catchment, which is located in the Kanda River basin Tokyo Metropolis, Japan, as shown in Fig. 5a. The study catchment will be termed "lower Ekota catchment" and Fig. 5b shows this catchment in some detail. The boundary of the study catchment is specified based on two conditions, the topography and the extension of the sewer pipe network. The lower Ekota catchment area is ~1.1 km^2 and the length of Ekota River inside it is ~1 km. It is essentially a residential area with some minor parks, groves, fields, etc. There are four water level gauges and one rainfall gauge in the catchment. Concerning the land use, ~60% of the surface is impervious. Along the lower Ekota River, between gauges L1 and L2, a regulating reservoir with side-spill weir exists on one side. Rainfall from the upper part of the Ekota catchment reaches the study

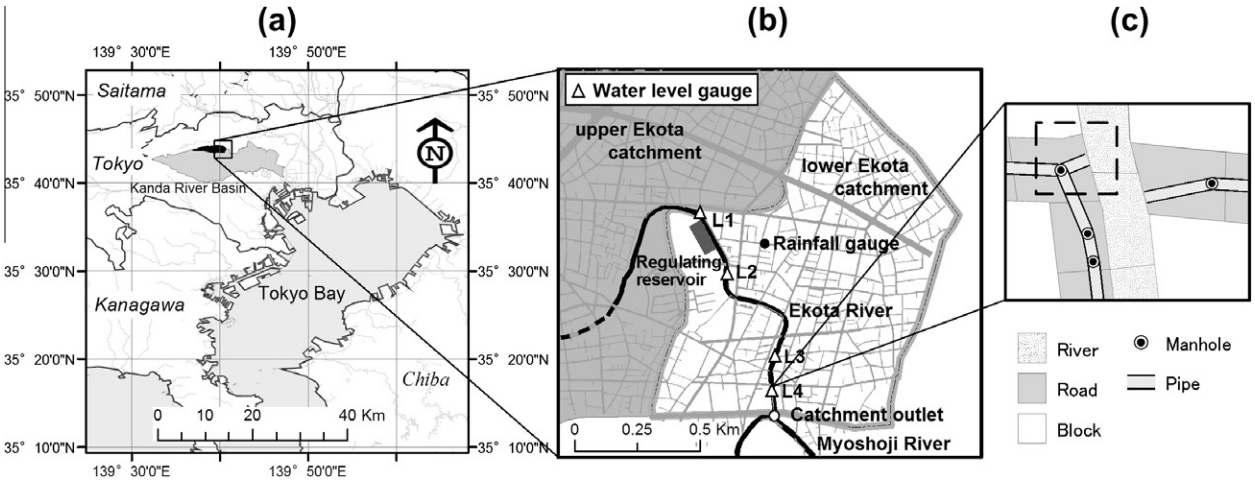

Fig. 5. Location of the Ekota catchment in Tokyo Prefecture, Japan (a), overview of the lower Ekota catchment (b) and map of he selected study location for detailed flow analysis (c).

catchment only by gravity flow through the combined sewer system. Along the Ekota River, there is a main sanitary sewer which connects the sewer pipe networks in the upper and lower Ekota catchment, respectively.

3.1. Urban landscape GIS delineation and model set-up

Table 1 shows the data sources used in the urban landscape GIS delineation performed when setting up the TSR model for the lower Ekota catchment. Fig. 6 illustrates the steps involved in urban landscape GIS delineation. Recently, vector-based basic GIS maps containing essentially the same information as urban databanks (Rodriguez et al., 2003) (except sewer system information) are becoming available also in major cities in Japan (Fig. 6a). The land use elements inside a block are manually added by use of topographic map (Fig. 6b). The road and block elements were divided into segments (Fig. 6d–e). The river segments were created with 20 m intervals because cross-sectional information was available with that spacing (Fig. 6f). The ground level of road and block segments were calculated as averages obtained from a 5 m DEM with 0.1 m precision in altitude (Fig 6g). The data on main pipes and junctions were obtained from the Tokyo government. The elevations of the manholes and the junctions were derived from the road segments (Fig. 6h). Finally, all elements created were combined to completely specify the catchment. Fig. 7 shows the final maps of surface component (a) and sewer element with road, block and river segments (b) in the entire study catchment. Table 2 shows the numbers and areas of the finally obtained GIS elements in the lower Ekota catchment. It should be emphasized that more than 9000 homogeneous elements (land use, road, river, manhole and pipe) were used to completely specify the small urban catchment.

3.2. Simulation of actual storm events

To test the applicability of the TSR model for storm runoff analysis, simulations were performed for two historical storm events. The first represents a small-scale event in which the storm water runoff in the sewer system was mainly free surface flow and no flooding occurred. The second event represents a major flooding, which followed heavy rainfall caused by the typhoon nr. 14 (Nagi) in September 2005. The resulting inundation is one of the most severe that has ever occurred in the Ekota catchment.

Table 1
Data sources required for advanced GIS delineation.

Data source (provider)	Contents of the data	Data type
Basic GIS delineation data (Toyo Met. Gov.)	Buildings, residential blocks and river	Polyline
Topographic paper map (Toyo Met. Gov.)	Land use information inside residential blocks	Paper
Channel cross section (Toyo Met. Gov., Bur. of Const.)	Channel cross sections	Paper
5 m DEM (Jpn. Geog. Surv. Inst.)	Elevation of road and block elements	Raster
Sewer pipe network data (Toyo Met. Gov., Bur. of Sewage)	Sewer pipe network	Vector

Concerning rainfall and runoff observations, there is one rainfall gauge in the catchment (Fig. 5b), where observations are made with a 1-min time resolution by the Tokyo Metropolitan Government. The gauge is of tipping-bucket type with a volume resolution of 0.5 mm. However, as it has been installed with the specific aim of observing high-intensity events for flood disaster prevention, time stamps are recorded only every second tip giving an effective volume resolution of 1 mm which is sufficient for the purpose. In a temporary measurement campaign carried out by the authors from 2005-08-20 to 2005-09-20, river water level was observed with a 2-min time resolution in four pressure-type water level gauges (L1–L4 in Fig. 5b). Model results can be obtained at arbitrary locations, but for comparison with observations the locations of gauges L2–L4 are used in the presentation of results below.

Table 3 shows the model parameters required. In this study, no attempt to calibrate or adjust parameter values is made but standard values are used. The initial loss parameters of impervious and pervious surfaces are obtained from Van de Ven et al. (1992), who reviewed urban drainage model parameters. The values of final infiltration capacity are obtained from Ando et al. (1986), who developed a flood runoff model for urban basins using measured final infiltration capacities of different land uses. Roughness coefficients are not easily estimated from the urban landscape GIS delineation data. Further field investigation is needed to identify the relationship between surface roughness and flow in surface elements. Therefore, published values of Manning's roughness coefficient n are used here. The value of roughness coefficient used for building flow is 0.035 (Yen, 1991). The values of n used for surface flow shown in Table 3 are obtained from Inoue et al. (1999). The values were estimated based on model simulations of flooding in a similar type of urban catchment in Japan. The values of n used

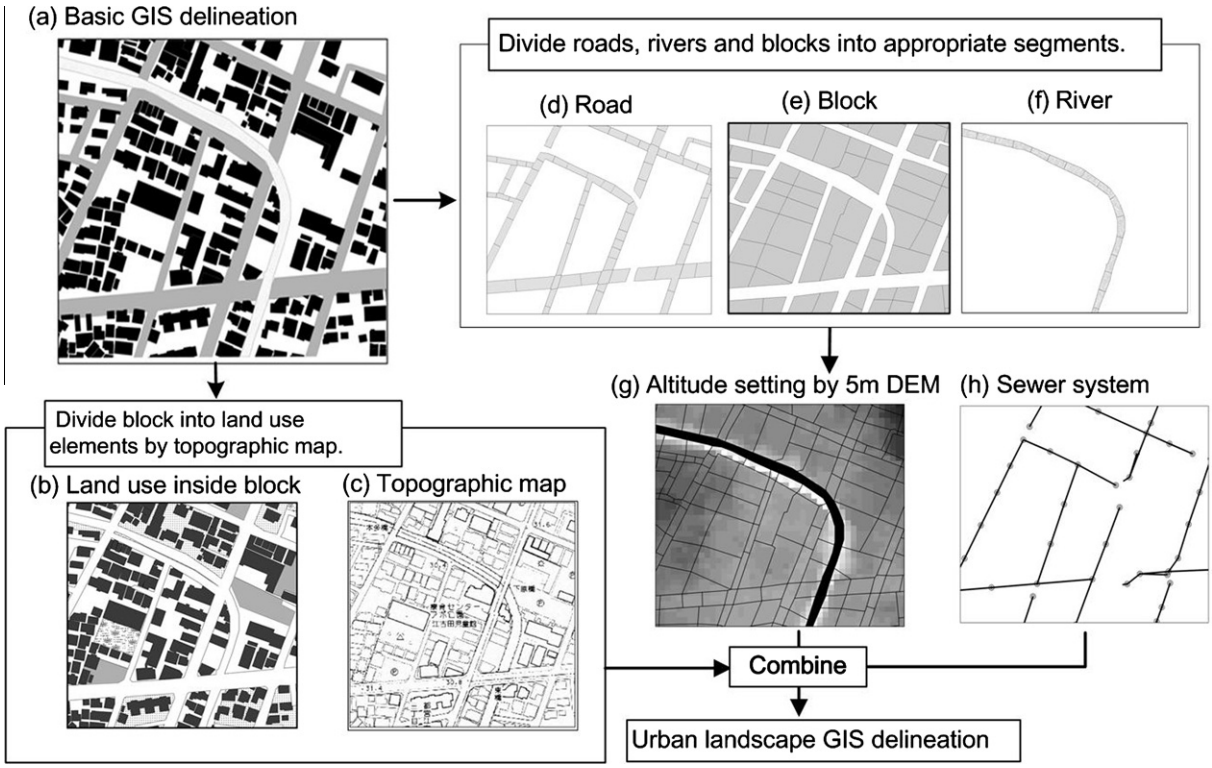

Fig. 6. Steps involved in the urban landscape GIS delineation.

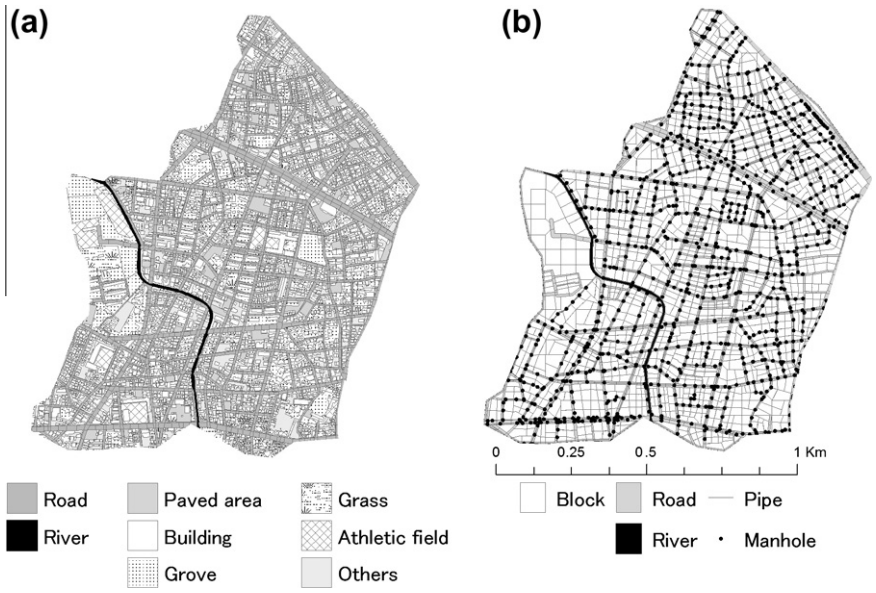

Fig. 7. Final map of surface component (a) and sewer element with road, block and river segments (b) in the lower Ekota catchment.

for sewer pipes and river channels are assigned as the standard roughness coefficient of concrete pipe and concrete channel, respectively (Mays, 2001).

In the simulations, the initial water levels and discharge in the river channel were set at stationary conditions after an adequate model warm-up period for calculation stability (1 h is enough in this catchment), during which river flow was calculated using the first water level observation in each event. The initial discharge in the combined sewer system, blocks and roads was set to zero. Concerning the boundary conditions for the main sanitary sewer, as it soon flows full and discharges downstream of the catchment during intense storms we assume that all water in the lower Ekota catchment pipe network flows out to the river. The river discharge at the upstream catchment border needs to be specified as a boundary condition. As a water level gauge exists at the upstream border, the boundary conditions here were estimated from a rating curve, calculated using observed water levels by taking into account the channel cross section and the average slope of the river bed. The water level at the catchment outlet was estimated from the calculated discharge using the outlet rating curve.

Table 2
Numbers of feature elements and their total element area.

Element name		Number	Total area (m^2)
Land use inside block	Paved area	58	44,542
	Building	4558	348,056
	Grove	174	205,088
	Athletic field	8	32,679
	Others	383	207,500
	Total	5181	873,865
Surface	Block	1,467	873,865
	Road	1,688	274,061
	River	53	8,063
	Total	3,208	1,155,989
Manhole		1,039	-
Pipe		1,053	-

Table 3
List of required input data and parameters of the model.

Parameter (unit)		Value
Initial loss L_i (mm)	Impermeable area	0.5
	Permeable area	1.0
Final infiltration capacity I_i (mm/h)	Grove	100.0
	Grass	20.0
	Athletic field	5.0
	Others	5.0
Building roughness coefficient n_b ($s/m^{1/3}$)		0.03
Surface roughness coefficient n ($s/m^{1/3}$)	Between roads	0.043
	Other	0.067
Channel roughness coefficient n ($s/m^{1/3}$)		0.0225
Pipe roughness coefficient n ($s/m^{1/3}$)		0.013

3.3. Event 8/25 (2005-08-25)

Observed and simulated water levels at gauge locations L2, L3 and L4 are shown in Fig. 5b, together with the observed rainfall during the event. At all three locations, the simulated levels overall agree very well with the observed ones although no calibration or tuning of model parameters was performed. This is supported by the RMSE, being in the range 5–8 cm (Table 4). The best performance is found at gauge L2, which is expected as this is located closest to the upstream catchment border and thus is most influenced by the boundary conditions there. Also the runoff peak at ~13:30 is overall well reproduced, although it is overestimated by 13 cm at gauge L3. Through rating curves, observed and simulated water levels were converted to discharge (not shown). Overall, the accuracy and tendency found were very similar to the results for water level.

The results shown in Fig. 8b and Table 4 include the runoff contribution from the upper Ekota catchment (Fig. 5b). As this subcatchment is larger than the lower Ekota catchment (Fig. 5a), this contribution from upstream has a significant influence on the total runoff in lower Ekota. Fig. 8c shows hydrographs from gauges L1, representing upstream inflow, and L4, representing total runoff. It is clear that upstream inflow is dominant, but also that the local

Table 4
Root Mean Square Error (RMSE) and peak level difference of events 2005-08-25 and 2005-09-04.

Location	Event 2005-08-25		Event 2005-09-04	
	RMSE for water level (m)	Peak level difference (m)	RMSE for water level (m)	Peak level difference (m)
L2	0.049	−0.03	0.133	−0.11
L3	0.077	0.13	0.192	−0.25
L4	0.069	0.02	0.160	−0.14

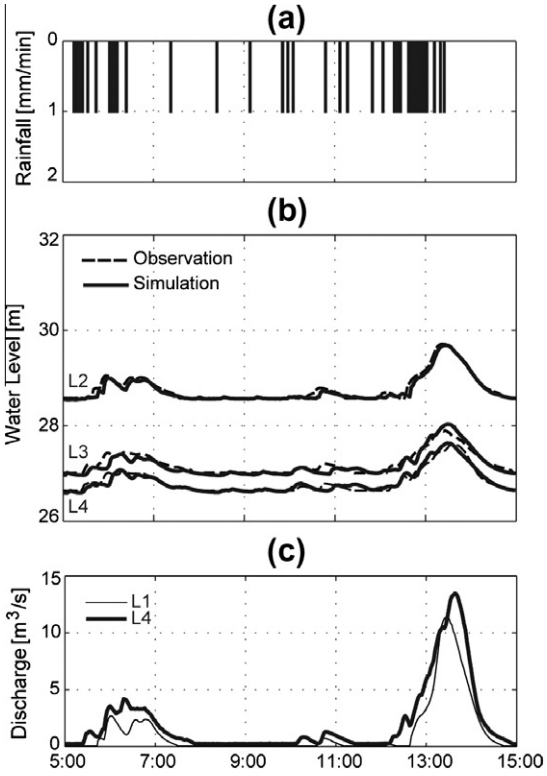

Fig. 8. Observed rainfall (a), observed and simulated river water level in gauges L2, L3 and L4 (b) and discharge in gauges L1 and L4 (c) during event 8/25.

contribution is not insignificant and therefore the close agreement in Fig. 8b would not have been attained without an accurate estimation of the local contribution by the TSR model. In the following, some properties of the locally generated runoff are presented and discussed. The objectives are to assess the realism of the results as well as to demonstrate what types of information the model is able to provide.

Fig. 9a shows rainfall intensity as 5-min accumulations to better visualize the rainfall event. Fig. 9b shows cumulative rainfall as well as cumulative runoff from all elements to the river channel. Fig. 9c shows time series of runoff to the river channel, both the underground flow through the sewer system and the surface flow from blocks and roads. In this event, there is almost no surface flow to the river. A negative value implies flow from the river channel to a sewer pipe, road or block element, but in this event no such reversed flow occurred. Fig. 9d shows time series of the total storage in sewer pipes, roads and blocks respectively. Throughout the relatively moderate rainfall event, most of the storage occurs in road elements. The sewer system storage, and to a lesser degree the road storage, directly reflects the rainfall intensity variations. As expected, the block storage is less variable.

As shown in Fig. 9b, the accumulated rainfall is 41 mm at the end of the event and the accumulated runoff to the river channel is 26 mm. In Fig. 9d, the total storage in all elements at the end of the simulation is found to be 2 mm. If these are regarded as direct runoff, the direct runoff ratio can be estimated as 0.69. Since the rate of impervious area in the study catchment is ~60%, and considering that rainfall on impervious surface is totally transformed into runoff, the direct runoff from pervious areas is estimated as ~9%.

To study in detail the flow conditions in a point where sewer pipe flow enters the river channel, the connection between pipe segment (with manhole segment) and river segment was selected as an example in Fig. 5c. Fig. 9e shows time series of the water level inside the manhole and the river channel as well as on the

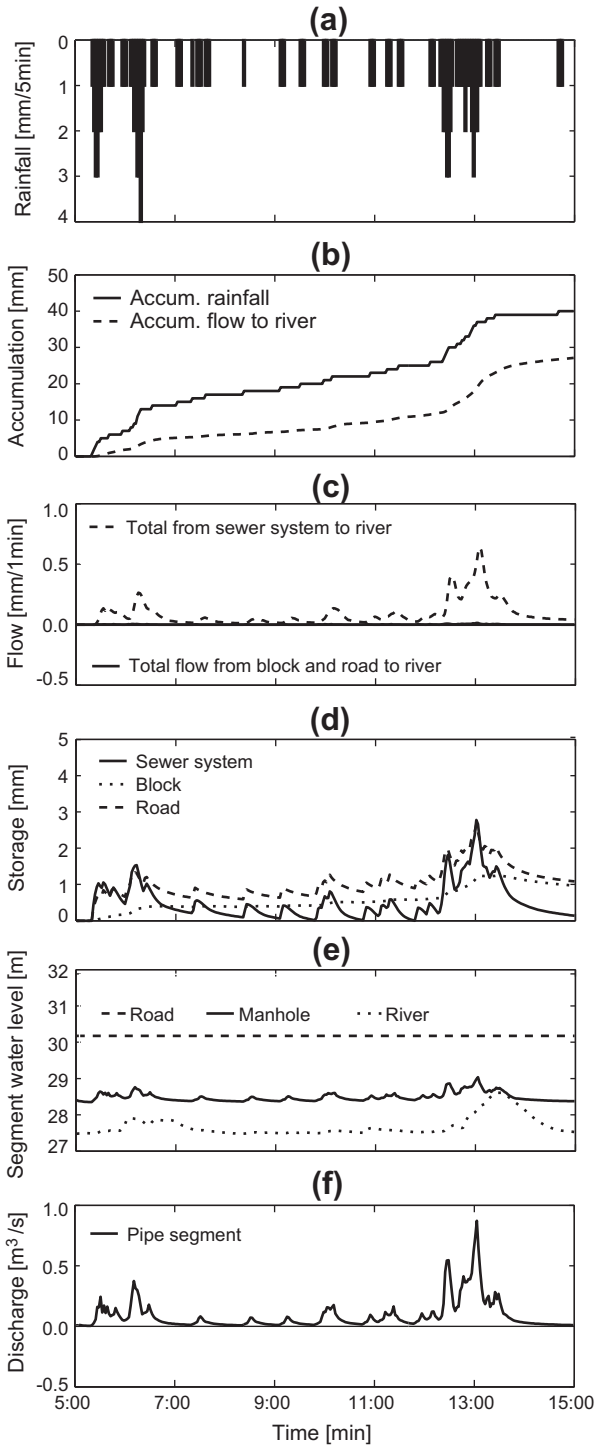

Fig. 9. Properties of rainfall and locally generated runoff during event 8/25: observed rainfall (a), accumulated observed rainfall and simulated flow to river (b), flow from sewer system, blocks and roads to river (c), storage in sewer, road and block element (d), water level in road segment, manhole segment and river segment (e) and discharge in pipe segment (f).

associated road segment. As expected, an increase of the water level in the river is preceded by an increase of the level in the manhole. In particular when the rainfall intensity is more than 2 mm/5 min, the manhole water level exhibits a clear increase which is followed by an increased river water level with some delay. Fig. 9f shows the time series of discharge in pipe segment. Basically, the discharge depends on the difference between the water levels in the manhole and in the river channel. During most of the event, the river water level is located below the lower pipe edge, i.e. the pipe flow is freely discharging into the river. In this situation, an increase of the manhole water level is directly reflected in an increased pipe discharge, but it is not sufficient for increasing the river water level up to the level of the pipe. Following the two rainfall peaks just before 13:00 (Fig. 6a), however, the pipe discharge peaks at nearly 1 m^3/s which makes the river water level increase above the upper pipe edge to almost reach the manhole level at ~13:30 (Fig. 9e). Because of the rapidly decreasing water level difference between the manhole and the river channel, also the pipe discharge finally decreases (Fig. 9f).

3.4. Event 9/4 (2005-09-04)

In order to evaluate also the model's ability to reproduce inundated conditions, a second runoff simulation was performed using a rainfall event occurring on 2005-09-04. On this day, typhoon nr. 14 in combination with a stationary front covering Japan produced a very heavy rainfall over the Ekota catchment as well as many other parts of Tokyo. Inside the Kanda River basin (Fig. 5a), the maximum observed 1-h rainfall volume was 112 mm and more than 2500 houses were damaged by flooding (Nomura, 2005).

In the model simulation, the initial and boundary conditions in the river, sewer, block and road elements are overall the same as for event 8/25. One exception concerns the boundary condition at the downstream end of the Ekota River. During event 9/4, flooding occurred in the junction of Ekota River and Myoshoji River (Fig. 5b) and all the neighboring areas were submerged. Also backflow occurred due to a higher water level in Myoshoji River than in Ekota River. Therefore the rating curve applied for event 8/25 could not be used. Instead, 1-min water level observations from 10 m downstream of the junction in the Myoshoji River are used as surrogate boundary conditions at the catchment outlet.

Figs. 10 and 11 show the same type of results as was shown for event 8/25 in Figs. 8 and 9. As shown in Fig. 10, the simulated water levels in all three locations considered agree well with the observed levels throughout the event. The RMSE is overall 2–3 times higher than in event 8/25, which is expected as the range of water level variation is higher with a similar order of magnitude in event 9/4. The runoff peak at ~23:30 is well reproduced but in this case systematically underestimated, by at most 25 cm at gauge L3. The agreement appears at least reasonable considering the extreme nature of the event and the fact that no parameter calibration or other form of model tuning was used.

The characteristics of runoff generated inside the lower Ekota catchment are displayed in Fig. 11. At the end of the event, the accumulated rainfall is 118 mm and the accumulated runoff 78 mm (Fig. 11b) and the total storage in all elements ~12 mm (Fig. 11d). The direct runoff ratio for this event becomes 0.77. This ratio is 8% higher than the ratio for event 8/25. The direct runoff from pervious areas is 17%, compared with 9% for event 8/25. Thus, as expected, the heavier the rainfall, the higher is the contribution to surface flow from pervious areas.

As shown in Fig. 11d, the storage in all sewer pipe elements is constantly ~7 mm during the main part of the rainfall event, when the intensity exceeds 4 mm/5 min. Even for higher intensities, the storage in the sewer system remains at ~7 mm. The reason is that the design rainfall used when constructing the sewer pipe system is ~50 mm/h. Thus, when the intensity exceeds 4 mm/5 min (48 mm/h), the water in the sewer system is surcharged to the surface elements. As shown in Fig. 11c, the flow from sewer, block and road elements to the river elements are sometimes negative during this event, particularly at ~23:30 following the third rainfall peak at ~23:00. Consequently the storage on road and block elements increases to reach their peak values around this time (Fig. 11d).

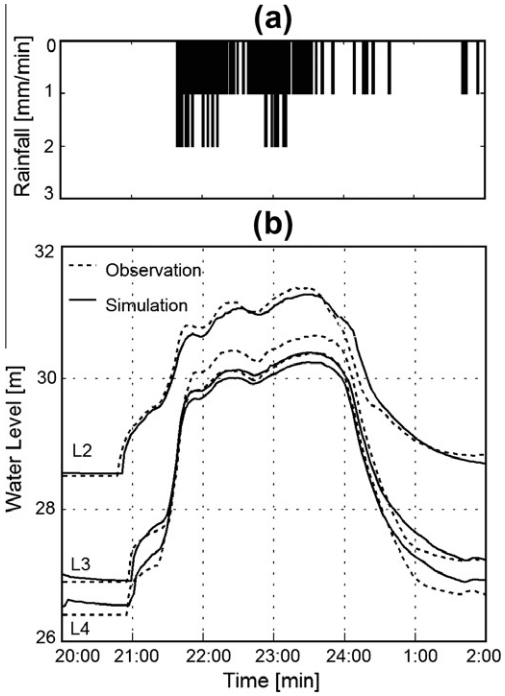

Fig. 10. Observed rainfall (a) and observed and simulated river water level in gauges L2, L3 and L4 (b) during event 9/4.

Besides the overflow from the river, additional storage is at this time produced by rainfall not able to flow out from the surface elements due to the inundated conditions. When rainfall intensity then decreases, the flow to the river returns to be positive, rapidly from blocks and roads and with some delay from the sewer system, and the storage decreases accordingly.

Concerning the example location (Fig. 5c), the water level in the river segment initially increases to approach the level in the manhole (Fig. 11e). This happens already before the start of the rainfall in the study catchments. The reason is the shape and direction of the rain band, which produced heavy rainfall west (i.e. upstream) of the catchment before reaching it. This affected the discharge in the lower Ekota River both by the increased inflow from the upper Ekota catchment and by backflow from Myoshoji River (Fig. 5b). Following the start of the rainfall at ~21:45, the water levels in both the manhole and the river abruptly increase as does the pipe discharge (Fig. 11f). At ~22:00 both the manhole and river water levels reach the level of the road. During the subsequent period of flooding, the water levels on the road, in the river and in the manhole are almost identical. However, although not clearly visible in Fig. 11e, the river water level becomes slightly higher than the road and manhole levels. This makes the pipe discharge negative for a 1.5-h period starting ~22:30 (Fig. 11f). Thus, during the period of flooding river water entered the road both through the pipe and as direct overflow from the river.

Fig. 11a–e shows the temporal evolution of the simulated inundation area during the event. At 22:00 some blocks starts to become inundated, in line with Fig. 12e. The main period of flooding is 23:00–24:00 and at 23:40 the volume of inundated water reached its peak. Because of the backflow from Myoshoji River, most of the inundated area was located close to the catchment outlet. The deepest inundation is found in the regulating reservoir (Fig. 5b), which was functioning normally throughout the event. Some inundation also occurred in a curved area just east of the catchment center. This area corresponds to the location of the main sewer pipe, which overflowed during the event. At 01:00, most of the inundated water had drained away.

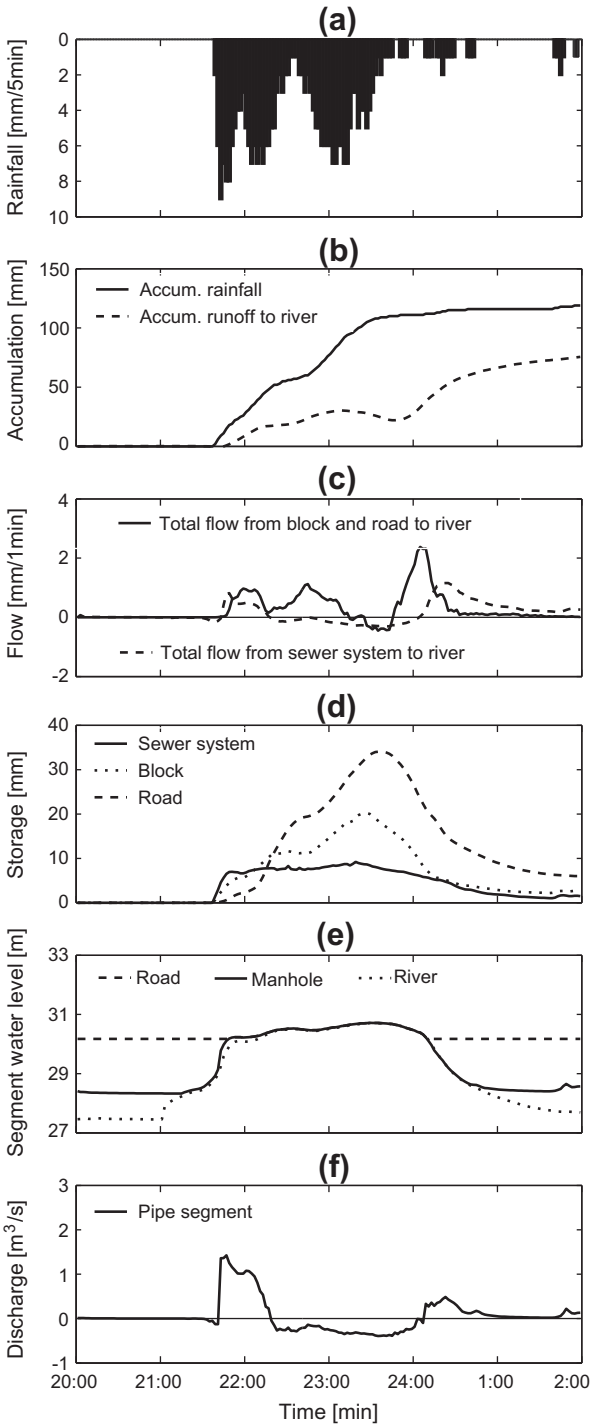

Fig. 11. Same diagrams as in Fig. 9 for event 9/4.

Fig. 12f shows the maximum extension of the inundated area, defined as the maximum inundation depth in each block or road element (>5 cm) during the flooding event. Showed in the figure is also a reported inundation area. This is based on a questionnaire that was distributed after the event, in which residents were asked to report damages caused by the flooding. As the area shown thus represents locations where damages were reported, and not any observed water depths, it must be considered only a rough estimate of the extension of the flooding. Even so, there is a reasonable agreement between simulated and reported inundation, with the reported area covering most of the locations that were severely inundated in the model simulation. No damages were reported

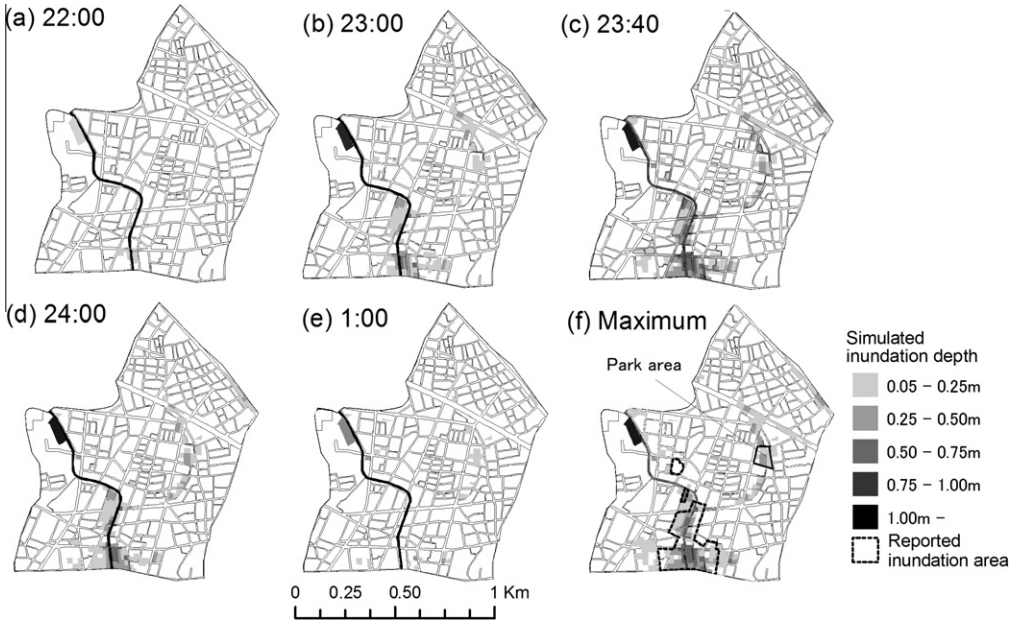

Fig. 12. Temporal evolution of the simulated inundated area during event 9/4 at times 22:00 (a), 23:00 (b), 23:40 (c), 24:00 (d) and 01:00 (e). Maximum extension of inundated area (f).

along the main sewer, which is at least partly owing to the existence of a large park in this area (Fig. 5b). This is designed to have a retention function during flooding events, and this function can thus be considered verified in Fig. 12f, indicating a water depth between 25 and 50 cm in the park. It may be remarked that no similar retention facility exists in the close vicinity of the catchment outlet, which could potentially have reduced the reported damages.

4. Summary and discussion

In this paper, a vector-based distributed storm event runoff model – the Tokyo Storm Runoff (TSR) model – was developed and tested for urban runoff analysis. The model was set up and evaluated for the small urban lower Ekota catchment (1.1 km^2), Tokyo Metropolis, Japan. The model was applied to simulate the runoff response to two historical storm events; one minor event resulting only in a small-scale flood wave and one major event which inundated parts of the catchment. No calibration or tuning was performed, but the general model formulation was used with standard parameter values obtained from the literature. For both events, the simulated water levels closely reproduced the observed ones. For the major event, also the reported inundation area was well described by the model. It was also demonstrated how the model can be used to evaluate the flow conditions in specific components of the urban hydrological system as well as to verify the function of flood-preventive structures.

In total, the results show that the suggested approach, based on a detailed reproduction of all relevant elements in an urban catchment, is able to simulate all aspects of urban flooding. Although in principle relatively straight-forward, this type of approach has until now not been practically attainable because of limitations in the resolution of available GIS data as well as limitations in computer power. We believe the methodology has a wide range of application for many practical problems such as evaluation of measures to improve flood protection facilities, which may include river channel improvements as well as installation of new runoff control facilities. Such proposed modifications may be easily implemented in the urban landscape GIS delineation and their function evaluated. Another potential use of the model is detailed urban impact assessment of the higher rainfall extremes that are commonly expected in the future. The high level of detail used in the reproduction of the catchment is further very useful as it facilitates communication of the results, which is important in light of the recent trend towards increased stakeholder involvement in hydrological modeling. The conditions at specific critical locations can be easily extracted from the model output and used during discussions with the stakeholders involved.

Finally, some issues related to future applications and development of the model will be discussed. A significant feature of the model is clearly its considerable data demand, both in terms of detailed GIS data on the urban environment and in terms of hydrological observations used for model validation. These data are seldom readily available today and it is crucial that the relevant authorities make efforts to compile high-resolution GIS data bases, e.g. urban databanks (e.g. Rodriguez et al., 2003), as well as to install and maintain observation stations. With comprehensive data for validation available it may be possible to further improve model performance and reliability by calibration of model parameters and/or by using more advanced hydrological and hydraulic model equations. One particular aspect of the data demand concerns the detailed land use information used in this application. This level of detail is seldom available even in today's urban GIS data. However, since basic GIS delineation data is usually available in most cities, it is possible to create the surface component including buildings, rivers, roads and other land uses. In the storm runoff simulation, the rate of imperviousness in other land use segments has to be estimated by calibration or other methods. To facilitate TSR model set-up in any urban catchment, automated procedures for division of land use segments inside block elements and for segmentation of roads and rivers are needed and such procedures are currently being developed.

Acknowledgements

We thank two reviewers for helpful comments on the original manuscript. Funding for the model development has been obtained

from the Japan Society for the Promotion of Science, by a Grant-in-Aid for Scientific Research (C) (Project Nr. 18560502, Head Investigator: Akira Kawamura). Funding from the Sasakawa Foundation, the Japan Society for the Promotion of Science, the Royal Swedish Academy of Sciences and the Mistra-SWECIA Programme allowed Jonas Olsson to visit Tokyo Metropolitan University. This support is gratefully acknowledged.

References

Abbott, M.B., Bathurst, J.C., Cunge, J.A., O'Connel, P.E., Rasmussen, J., 1986a. An introduction to the European Hydrological System – Systeme Hydrologique Europeen, "SHE", 1: History and philosophy of a physically-based, distributed modelling system. J. Hydrol. 87, 45–59.

Abbott, M.B., Bathurst, J.C., Cunge, J.A., O'Connel, P.E., Rasmussen, J., 1986b. An introduction to the European Hydrologic System – System Hydrologique Europeen, "SHE" 2: Structure of a physically based, distributed modeling system. J. Hydrol. 87, 61–77.

Andjelkovic, I., 2001. Guidelines on Non-structural Measures in Urban Flood Management. International Hydrological Programme, Technical Document in Hydrology, No. 50.

Ando, Y., Takahashi, Y., Izumi, K., Kanno, K., 1986. Urban flood modeling considering infiltration various land uses. In: Maksimović, Č., Radojković, M. (Eds.), Urban Drainage Modelling. Pergamon Press, Oxford, England.

Balloffet, A., 1969. One-dimensional analysis of floods and tides in open channels. J. Hydaul. Div. Proc. ASCE 95 (HY4), 1429–1450.

Beven, K.J., Kirkby, M.J., Schoffield, N., Tagg, A., 1984. Testing a physically based flood forecasting model (TOPMODEL) for three UK catchments. J. Hydrol. 69, 119–143.

Bornstein, R., Lin, Q., 2000. Urban heat islands and summertime convective thunderstorms in Atlanta: three case studies. Atmos. Environ. 34, 507–516.

Choi, K.S., Ball, E.B., 2002. Parameter estimation for urban runoff modeling. Urban Water (4), 31–41.

Dey, A.K., Kamioka, S., 2007. An integrated modeling approach to predict flooding on urban basin. Water Sci. Technol. 55. doi:10.2166/wst.2007.091.

Dronkers, J.J., 1969. Tidal computations for rivers, coastal areas, and seas. J. Hydraul. Div., Proc. ASCE 95 (HY1), 29–78.

Ettrich, N., Steiner, K., Thomas, M., Pothe, R., 2005. Surface models for coupled modelling of runoff and sewer flow in urban areas. Water Sci. Technol. 52, 25–33.

Genovese, E., 2006. A Methodological Approach to Land Use-based Flood Damage Assessment in Urban Areas: Prague Case Study. Mission of the Institute for Environment & Sustainability, European Commission.

Goto, K., 2000. Two underground accidents of urban flooding. Jpn. Soc. Civ. Eng. 85 (6), 66–69 (in Japanese).

Hsu, M.H., Chen, S.H., Chang, T.J., 2000. Inundation simulation for urban drainage basin with storm sewer system. J. Hydrol. 234. doi:10.1016/S0022-1694(00)00237-7.

Hydrologic Engineering Center (HEC), 1998. HEC-1 Flood Hydrograph Package, User's Manual, CPD-1A, version 4.1. US Army Corps of Engineers, Davis, CA, 434 p.

Inoue, K., Kawaike, K., Toda, K., 1999. Refuge analysis under storm surge based on the street network model. In: Pro. '99 Int. Symp. on Flood Cont., Beijing, China, pp. 507–514.

IPCC, 2007. Summary for Policymakers. Contribution of Working Group II to the Fourth Assessment Report of the Intergovernmental Panel on Climate Change, 2007.

Kusuda, T., 1999. 1999.6.29 Fukuoka Storm. Jpn. Soc. Civ. Eng. 84 (11), 42–44 (in Japanese).

Leopold, L.B., 1968. Hydrology for Urban land Planning. US Geological Survey Circular, vol. 554, pp. 1–18.

Mays, L.W., 2001. Water Resources Engineering. John Wiley and Sons, US.

Niehoff, D., Fritsch, U., Bronstert, A., 2002. Land-use impacts on storm-runoff generation: scenarios of land-use change and simulation of hydrological response in meso-scale catchment in SW-Germany. J. Hydrol. 267, 80–93.

Nomura, T., 2005. Flood damage caused by local downpour in Tokyo. Jpn. Soc. Civ. Eng. 90 (11), 51–52 (in Japanese).

Park, S.Y., Lee, K.W., Park, I.H., Ha, S.R., 2008. Effect of the aggregation level of surface runoff fields and sewer network for a SWMM simulation. Desalination 226, 328–337.

Pilgrim, D.H., Cordery, I., 1992. Flood runoff. In: Maidment, D.R. (Ed.), Handbook of Hydrology. McGraw-Hill, New York, US (Chapter 9).

Preissmann, A., Cunge, JA., 1961. Calcul des intumescences sur machinas electroniques. In: Pro. 9th Cong. of IAHR, Dubrovnik, Yugoslavia, pp. 656–664.

Rodriguez, F., Andrieu, H., Creutin, J.D., 2003. Surface runoff in urban catchments: morphological identification of unit hydrographs from urban databanks. J. Hydrol. 283. doi:10.1016/S0022-1694(03)00246-4.

Rodriguez, F., Andrieu, H., Morena, F., 2008. A distributed hydrological model for urbanized areas – model development and application to case studies. J. Hydrol. doi:10.1016/j.jhydrol.2007.12.007.

Sample, D.J., Heaney, J.P., Wright, L.T., Koustas, R., 2001. Geographic information systems, decision support systems, and urban storm-water management. J. Water Resour. Plan. Manage. ASCE 127 (3), 155–161.

Singh, V.P., 1995. Watershed modeling. In: Singh, V.P. (Ed.), Computer Models of Watershed Hydrology. Water Resources Publications, Colorado, US (Chapter 1).

Singh, V.P., 1996. Kinematic Wave Modeling in Water Resources. John Wiley & Sons, USA.

Smith, M.B., 1992. A GIS-based distributed parameter hydrologic model for urban areas. Hydrol. Process. 7, 45–61.

Smith, M.B., 2006. Comment on 'Analysis and modeling of flooding in urban drainage systems'. J. Hydrol. 317. doi:10.1016/j.jhydrol.2005.05.027.

Spears, D.D., 1995. SSARR model. In: Singh, V.P. (Ed.), Computer Models of Watershed Hydrology. Water Resources Publications, Colorado, US (Chapter 11).

Sugawara, M., 1974. Tank Model with Snow Component. National Research Center for Disaster Prevention, Japan.

Szöllösi-Nagy, A., Zevenbergen, C., 2004. Urban Flood Management. Taylor & Francis Publishers, London (UK).

Toyokuni, E., Watanabe, M., 1986. Urban flood modeling considering infiltration various land uses. In: Maksimović, Č., Radojković, M. (Eds.), Urban Drainage Modelling. Pergamon Press, Oxford, England.

Van de Ven, F.M.H., Nelen, A.J.M., Geldof, G.D., 1992. Urban drainage. In: Smart, P., Herbertson, J.G. (Eds.), Drainage Design. Blackie, New York, US (Chapter 5).

Yamamoto, H., Iwaya, K., 2002. Characteristics of heavy rainfall and flood damage in Aichi prefecture from September 11th to 12th 2000. J. Natural Disaster Sci. 24 (1), 15–24.

Yen, B.C., 1991. Hydraulic resistance in open channel. In: Yen, B.C. (Ed.), Channel Flow Resistance: Centennial of Manning's Formula. Water Resources Publications, Colorado, US.